Oscillator strength and linewidth measurements of dipole-allowed transitions in $^{14}N_2$ between 93.5 and 99.5 nm

G. Stark[a)]
Department of Physics, Wellesley College, Wellesley, Massachusetts 02481

K. P. Huber
Steacie Institute for Molecular Sciences, National Research Council of Canada, Ottawa, Ontario K1A 0R6, Canada

K. Yoshino and Peter L. Smith
Harvard-Smithsonian Center for Astrophysics, Cambridge, Massachusetts 02138

K. Ito
Photon Factory, Institute for Materials Structure Science, High Energy Accelerator Research Organization, 1-1 Oho, Tsukuba, Ibaraki 305-0801, Japan

(Received 1 September 2005; accepted 12 October 2005; published online 2 December 2005)

Line oscillator strengths in 16 electric dipole-allowed bands of $^{14}N_2$ in the 93.5–99.5 nm (106 950–100 500 cm^{-1}) region have been measured at an instrumental resolution of 6.5×10^{-4} nm (0.7 cm^{-1}). The transitions terminate on vibrational levels of the $3p\sigma\ ^1\Sigma_u^+$, $3p\pi\ ^1\Pi_u$, and $3s\sigma\ ^1\Pi_u$ Rydberg states and of the $b'\ ^1\Sigma_u^+$ and $b\ ^1\Pi_u$ valence states. The J dependences of band f values derived from the experimental line f values are reported as polynomials in $J'(J'+1)$ and are extrapolated to $J'=0$ in order to facilitate comparisons with results of coupled-Schrödinger-equation calculations that do not take into account rotational interactions. Most bands in this study reveal a marked J dependence of the f values and/or display anomalous P-, Q- and R-branch intensity patterns. These patterns should help inform future spectroscopic models that incorporate rotational effects, and these are critical for the construction of realistic atmospheric radiative transfer models. Linewidth measurements are reported for four bands. Information provided by the J dependences of the experimental linewidths should be of use in the development of a more complete understanding of the predissociation mechanisms in N_2. © *2005 American Institute of Physics*.
[DOI: 10.1063/1.2134703]

I. INTRODUCTION

Molecular nitrogen figures prominently in the photochemistry of the Earth's upper atmosphere, where photoexcitation in the extreme ultraviolet (EUV) spectral region ($\lambda<100$ nm) and electron-impact excitation initiate critical dissociation and ionization processes. Strong airglow emissions in the EUV and the vacuum ultraviolet (VUV) ($\lambda>100$ nm) are observed in the terrestrial atmosphere[1–3] as well as in the N_2-rich atmospheres of Titan[4–6] and Triton,[7] and N_2 was recently identified in the interstellar medium through its EUV absorption signature.[8] The quantitative interpretation of atmospheric and interstellar observations and the modeling of upper atmospheric processes require a detailed understanding of the EUV photoabsorption spectrum of N_2. In particular, EUV transmission models through N_2-rich atmospheres[9,10] and radiative transfer models for the interpretation of upper atmospheric airglow observations[6] require a comprehensive and complete database of line positions, line oscillator strengths, and linewidths. Despite considerable experimental and theoretical efforts, significant uncertainties and gaps remain in the spectroscopic database, including the fundamental parameters such as line oscillator strengths and line widths. In this paper we report measured line oscillator strengths in sixteen bands of $^{14}N_2$ in the 93.5–99.5 nm(106 950–100 500 cm^{-1}) region as well as measured linewidths in four bands. In the notation used throughout this paper, these are the transitions between the ground state $X(0)$ and the vibronic upper states $b(0-8)$, $b'(1,4)$, $c_4'(0,1)$, $c_3(0,1)$, and $o_3(0)$.

The complex electric dipole-allowed absorption spectrum of N_2 shortward of 100 nm was first interpreted by Lefebvre-Brion,[11] Dressler,[12] and Carroll and Collins[13] as arising from transitions to the strongly perturbed vibrational progressions of three Rydberg and two valence states. $c_4'\ ^1\Sigma_u^+$ and $c_3\ ^1\Pi_u$ are the $n=3$ lowest members of the $np\sigma$ and $np\pi$ Rydberg series converging to the $X\ ^2\Sigma_g^+$ ground state of N_2^+; the $o_3\ ^1\Pi_u$ state is the $n=3$ lowest member of the $ns\sigma$ series converging to $A\ ^2\Pi_u$ of N_2^+; and $b\ ^1\Pi_u$ and $b'\ ^1\Sigma_u^+$ are valence states. A comprehensive treatment of the homogeneous Rydberg-Rydberg and Rydberg-valence interactions by Stahel *et al.*[14] successfully reproduced the strikingly anomalous absorption strength patterns within the vibrational progressions. Stahel *et al.*[14] used observed vibronic term values and rotational constants[15–17] together with relative dipole strengths determined from electron-energy-loss spectra[18] to optimize a set of electronic transition moments derived from

[a)]Electronic mail: gstark@wellesley.edu

electronically coupled diabatic potential curves. Spelsberg and Meyer[19] recently refined the analysis by combining *ab initio* calculated potential curves with *R*-dependent electronic couplings, producing an impressive agreement not only with the observed rovibronic energies, but also with the observed dipole strength distribution.[18]

Predissociation effects in the N_2 EUV absorption spectrum vary dramatically from band to band. The clarification of the underlying mechanisms has been a long-standing unresolved problem. Building on earlier works,[12,13,20,21] Lewis *et al.*[22] have developed a quantitative predissociation model for the b, c_3, and $o_3\ ^1\Pi_u$ states. A coupled-channel Schrödinger-equation model of their interactions with the C and $C'\ ^3\Pi_u$ states, optimized using the available experimental database of isotope-dependent line positions and linewidths, reproduces all but the rotation-dependent line broadenings observed in the $^{14}N_2$, $^{15}N_2$, and $^{14}N^{15}N\ ^1\Pi_u$ vibrational levels below 105 350 cm^{-1}. The model calculation shows that the spin-orbit interaction of the $b\ ^1\Pi_u$ and $C\ ^3\Pi_u$ levels along with an electrostatic interaction between the C state and the continuum of $C'\ ^3\Pi_u$ accounts for the observed line broadening patterns.

Early measurements of N_2 band oscillator strengths at EUV wavelengths were carried out by Carter,[23] Gürtler *et al.*,[24] and Lawrence *et al.*[25] at a relatively low resolution of $\approx 5\ cm^{-1}$. In principle, optical-absorption measurements provide a direct determination of oscillator strengths. However, an insufficient instrumental resolution complicates the analysis of strongly absorbed lines.[26–28] The effects associated with an insufficient instrumental resolution, if not minimized or properly accounted for, result in a systematic underestimation of integrated photoabsorption cross sections and f values. Various strategies can be used to minimize instrumental effects in an absorption measurement. However, there are unavoidable uncertainties associated with extracting f values from low-resolution absorption measurements, and these uncertainties increase with decreasing instrumental resolving power.

Stark *et al.*[29] reported oscillator strengths for seven N_2 bands between 95.8 and 99.4 nm from absorption spectra recorded with an instrumental resolution of $\approx 0.7\ cm^{-1}$, a sevenfold improvement over previous measurements. To minimize instrumental resolution effects, these measurements were limited to peak optical depths of $\leqslant 0.3$, and corrections based on the analyses of synthetic absorption spectra convolved with the estimated instrumental line shape were applied to the measured band-integrated cross sections. Because of the continued interest in the detailed spectroscopy of the strong $c_4'(0)-X(0)$ transition at 95.9 nm (104 270 cm^{-1}), Stark *et al.*[30] remeasured the band's absorption spectrum, focusing on the determination of individual line f values. A least-squares line-profile fitting technique was used to account for instrumental resolution effects.

N_2 band f values have also been derived from electron-scattering measurements. Geiger and Schröder[18] reported relative intensities in the N_2 energy-loss spectrum of 25 keV electrons at a resolution of 10 meV($\approx 80\ cm^{-1}$); after correction for the scattering geometry, these intensities can be converted to relative band oscillator strengths.[14] Chan *et al.*[31] determined absolute N_2 band f values from energy-loss spectra of 8 keV electrons at a resolution of 48 meV ($\approx 400\ cm^{-1}$). Ajello *et al.*[32] reported a $c_4'(0)-X(0)$ band f value derived from electron-impact studies of the emission-excitation cross section for the $c_4'(0)$ level.

Evidence for predissociation line broadening in a number of $b(v)^1\Pi_u-X(0)$ bands was described by Carroll and Collins[13] in their photographic survey of the N_2 EUV absorption spectrum. The first quantitative estimates of N_2 linewidths were reported by Leoni and Dressler[20] from photoelectric absorption measurements and by Oertel *et al.*[33] from fluorescent decay following synchrotron-radiation excitation. This earlier work has been supplanted by an extensive program of laser-based linewidth and lifetime measurements by Ubachs and co-workers.[34–41]

The strong Rydberg-Rydberg, Rydberg-valence, and valence-valence interactions among the singlet and triplet states also produce conspicuous rotation-dependent effects on line strengths and linewidths. Carroll and Collins[13] identified a number of anomalous line-strength patterns in $b(v)-X(0)$ bands. J-dependent line oscillator strengths were reported for the $c_4'(0)-X(0)$ band by Stark *et al.*[30] Walter *et al.*[42] reported extreme departures from normal rovibrational intensity patterns in photofragment signals following laser excitation of the $c_4'(3,4)$, $c_3(3,4)$, and $b'(10,13)$ levels. Rotation-dependent linewidths were reported for the $c_4'(4)$, $c_3(4)$, and $b'(13)$ levels,[43] and rotation-dependent lifetimes were reported for the $c_4'(0)$ and $c_4'(2)$ levels.[38] Ajello *et al.*,[44] Shemansky *et al.*,[45] and Liu *et al.*[46] derived J-dependent predissociation yields in the $c_4'(0,3,4)$ levels from emission intensities following electron-impact excitation. Heterogeneous interactions must be included in models to account for many of the rotation-dependent effects. Edwards *et al.*[47] extended the study of Stahel *et al.*[14] by including the effects of rotation, and they discussed the consequences of the heterogeneous mixing of Rydberg- and valence-state rovibronic levels on the intensity distribution in emission spectra. References 32, 38, 42, and 43 used similar methods to interpret the observed J dependences of lifetimes, linewidths, and predissociation yields.

Given the strength and complexity of the interactions involving singlet and triplet states of N_2, J-dependent effects such as those already reported can be expected to be widespread throughout the near-threshold region of N_2. A more complete database of J-dependent effects will inform the continued modeling of the N_2 rovibronic structure. The J dependences of the line oscillator strengths and linewidths reported in this paper have, where possible, been extrapolated to $J'=0$; these extrapolated values can be directly compared with f values and linewidths predicted by coupled-Schrödinger-equation molecular models[14,19,22] that do not account for rotational effects. The accompanying paper by Haverd *et al.*[48] presents a refined coupled-Schrödinger-equation model of the low-lying $^1\Pi_u$ and $^3\Pi_u$ states of N_2 that accounts for many of the rotational effects reported here. Nevertheless, the extent of the J dependence of N_2 oscillator strengths and linewidths in the EUV region remains to be fully investigated and explained.

II. EXPERIMENTAL PROCEDURE

The photoabsorption measurements reported here were part of a three-year effort to record high-resolution, room-temperature spectra of all dipole-allowed N_2 transitions in the 86–100 nm (116 300–100 000 cm^{-1}) region. All f values and linewidths were derived from measurements made at the 2.5 GeV storage ring of the Photon Factory, a synchrotron-radiation facility at the High Energy Accelerator Research Organization in Tsukuba, Japan. A 6.65 m spectrometer with a focal plane scanner[49,50] was used to provide high spectral resolution. The bandpass of the continuum radiation entering the spectrometer was reduced to about 3 nm by a zero-dispersion order sorter. A 1200 groove mm^{-1} grating, blazed at 550 nm, was used in the sixth order to give a reciprocal dispersion of ≈ 0.02 nm mm^{-1}. Spectrometer entrance and exit slits of ≈ 10 μm resulted in an instrumental resolution of about 6.5×10^{-4} nm(0.70 cm^{-1}). The determination of the instrument profile is discussed in Sec. III.

The spectrometer tank, at a temperature of 295 K, served as an absorption cell with a path length of ≈ 12.5 m; the exact value depends on the grating position and was calculated for each absorption band. N_2 was used in natural isotopic abundance ($^{14}N_2$, 99.3%; $^{14}N^{15}N$, 0.7%). The strengths of the 16 measured $^{14}N_2$ bands vary widely, requiring a correspondingly wide range of column densities. Absorption spectra were recorded at tank pressures ranging from 7.9×10^{-7} to 1.5×10^{-4} torr, corresponding to N_2 column densities ranging from 3.3×10^{13} to 6.2×10^{15} cm^{-2}. At the lower pressures, outgassing from the tank walls would have contaminated a static gas sample over the time of a full scan. Consequently, a flowing configuration was used. The spectrometer tank was continuously pumped by a 1500 liters/s turbomolecular pump, while N_2 entered the tank through a needle valve. At the pressures used, molecular flow conditions prevailed, ruling out the occurrence of pressure differentials that could have adversely affected the measurements.

The spectrometer tank pressure was monitored with an ionization gauge. The limiting pressure in the tank was $\approx 2.0\times10^{-7}$ torr; the composition of the residual gas was unknown, but the tank contents at this limiting pressure showed no signs of absorption in the wavelength region studied. For pressures greater than 2×10^{-6} torr, the ionization gauge was calibrated by volumetric expansion of N_2; a small volume, representing a measured fraction of the spectrometer tank volume and filled to pressures that could be measured with a capacitance manometer, was expanded into the main tank. For the small fraction of scans taken at pressures below 2×10^{-6} torr, volumetric expansion becomes unreliable because of increasing uncertainties in the capacitance manometer readings and because of the increasing importance of spectrometer tank outgassing. The column density calibration in this pressure region is described in Ref. 30.

Bands with sharp rotational features were scanned at speeds ranging from 0.0025 nm min^{-1} to 0.006 nm min^{-1}; signal integration times of about 1 s then resulted in one data point for each 4.4×10^{-5}–1.06×10^{-4} nm interval of the spectrum. For the $b(3)-X(0)$ band, the diffuseness of the rotational lines allowed the detector scanning speed to be increased to 0.015 nm min^{-1}. Most bands were scanned in two or three overlapping portions, typically of width 0.1 nm. Signal rates from the detector, a windowless solar-blind photomultiplier tube with a CsI-coated photocathode, were about 50 000 s^{-1} for the background continuum; the detector dark-count rate was less than 2 s^{-1}. To define the background continuum level, the wavelength limits of each individual scan were chosen to include regions of negligible N_2 absorption. Typically, a signal-to-noise ratio of about 250 was achieved for the continuum level.

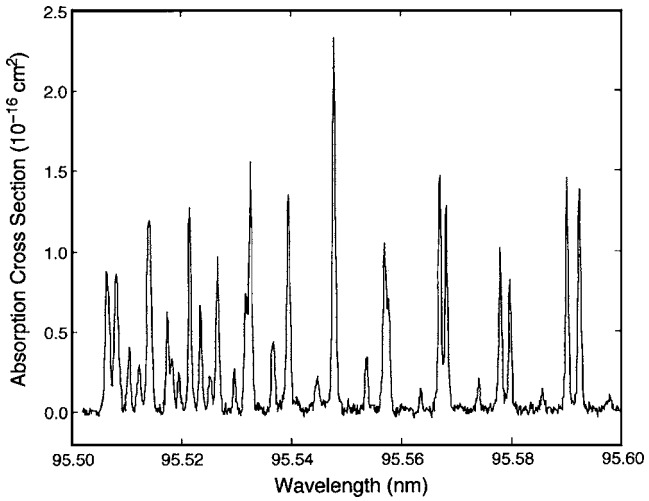

FIG. 1. Representative measured photoabsorption cross section of the $b(5)-X(0)$ bandhead region at 295 K. Because of instrumental distortion of the lines, the measured peak cross sections are lower limits to the correct values (see text).

III. ANALYSES

A total of 81 absorption scans were recorded, at a variety of N_2 column densities, of the 16 bands analyzed in this paper. The absorption spectra were first converted to *measured* absorption cross sections through application of the Beer-Lambert law,

$$\sigma_{\mathrm{exp}}(\lambda) = \frac{1}{N}\ln\left[\frac{I_0(\lambda)}{I(\lambda)}\right], \tag{1}$$

where $\sigma_{\mathrm{exp}}(\lambda)$, the experimental absorption cross section, includes the effects of the finite instrument resolution; N is the column density of N_2 molecules; $I_0(\lambda)$ is the background continuum level; and $I(\lambda)$ is the transmitted intensity. A correction for scattered light in the spectrometer, known to be less than 3% of $I_0(\lambda)$,[50] was not applied to the data. To illustrate the general quality of the data, a measured absorption cross section of the bandhead region of the $b(5)-X(0)$ band is shown in Fig. 1.

For each unblended line within a band, a least-squares fitting routine that accounts for the effects of the finite instrumental resolution was used to determine a value for the corrected integrated cross section. The background continuum level was established by sampling regions of negligible absorption between lines. Any variations in $I_0(\lambda)$ across individual lines were modeled in the fits by linear interpolation. All rotational lines were modeled with Voigt profiles. The

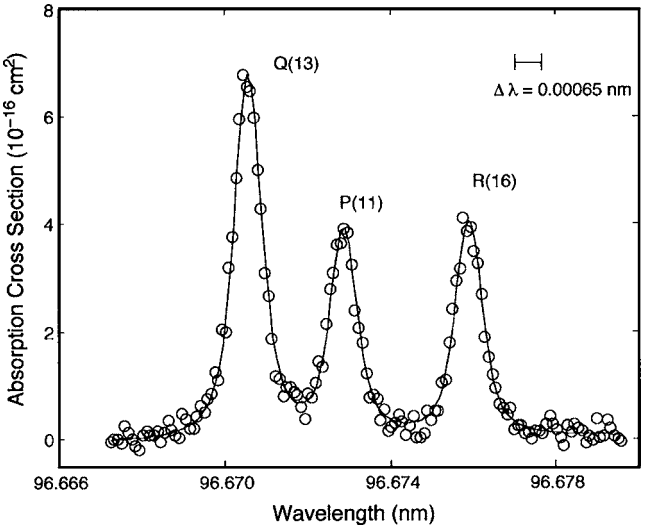

FIG. 2. Open circles: measured photoabsorption cross sections of the $Q(13)$, $P(11)$, and $R(16)$ lines in the $b(4)-X(0)$ band. Solid line: modeled cross sections from a least-squares fit. The instrument resolution (FWHM) is also indicated.

Gaussian component is the room-temperature Doppler width of 0.24 cm^{-1} full width at half maximum (FWHM). For bands with appreciably broadened lines (Lorentzian component >0.10 cm^{-1} FWHM), the Lorentzian component of each rotational line profile was determined from the least-squares fit [the strongly broadened $b(3)-X(0)$ band was analyzed differently; see Sec. IV]. For all other bands, the relatively narrow Lorentzian component could not be unambiguously determined from our data. In these cases, the published values of Ubachs,[36] Ubachs *et al.*[37,38] and Sprengers *et al.*[39–41] were used to fix the Lorentzian component in the fitting routine.

The instrument function was also represented by a Voigt profile. Its parameters were determined by least-squares fits to the unblended lines of the $b(1)-X(0)$ and $c_4'(0)-X(0)$ bands. The upper levels of these two bands show minimal broadening due to predissociation, and with Lorentzian linewidths of 0.002 and 0.007 cm^{-1},[38,39] respectively, the line shapes are almost pure Gaussians. As the analyzed absorption scans were recorded over a three-year period, the instrument function was checked periodically to account for possible drifts in the optical alignment and in the slit widths of the spectrometer. Two instrument profiles were adopted for the data sets in this paper: one was constructed from a Gaussian width of 0.56 cm^{-1} and a Lorentzian width of 0.25 cm^{-1}, producing an instrumental FWHM of 0.71 cm^{-1}; the other was constructed from widths of 0.62 and 0.21 cm^{-1}, producing a FWHM of 0.73 cm^{-1}. From the distribution of fitting results, we estimate that the Gaussian and Lorentzian components of the adopted instrument Voigt profiles have uncertainties of about ±0.04 and ±0.09 cm^{-1}, respectively. The uncertainties are correlated such that the instrument Voigt functions have total uncertainties of ±0.05 cm^{-1}.

A representative fit to three rotational lines in the $b(4)-X(0)$ band is shown in Fig. 2 along with an indication of the FWHM of the assumed instrument profile. The integrated cross sections of individual rotational lines, determined from the fitting procedure, were converted into line oscillator strengths according to[51]

$$f_{J',J''} = \left(\frac{4\varepsilon_0 m_e c^2}{e^2}\right)\frac{\int\sigma(\lambda)d\lambda}{\lambda^2\alpha_{J''}} = (1.1296\times 10^3)\frac{\int\sigma(\lambda)d\lambda}{\lambda^2\alpha_{J''}}, \quad (2)$$

where $\sigma(\lambda)$ and λ are measured in units of 10^{-16} cm^2 and nanometers, respectively, and $\alpha_{J''}$ is the fractional population of N_2 molecules in the J'' rotational level as determined from a normalized Boltzmann factor based on N_2 ground-state term values[52] and taking into account the 2:1 statistical weights of even- and odd-numbered levels due to nuclear spin. All final line f values and linewidths are weighted averages of results determined from absorption measurements of at least two different N_2 column densities. To minimize errors associated with uncertainties in the adopted instrument profile, only absorption features with measured peak optical depths <0.5 were included in the weighted averages.

The uncertainties in the N_2 column densities, the adopted instrument profile of the spectrometer, and the parameters extracted from the least-squares fitting routine all contribute to the estimated uncertainties in individual line f values and widths. In addition, the uncertainties in the adopted linewidths for features with Lorentzian components less than 0.1 cm^{-1} FWHM, taken from literature,[36–41] contribute to line f value uncertainties in a subset of the bands. Column density uncertainties are estimated to range from about 5% for the highest-pressure scans to about 15% for the lowest-pressure scans, where outgassing effects become significant and pressure calibrations are more susceptible to systematic error. The uncertainties in the adopted instrument profiles, discussed above, produce f-value uncertainties that range from ≈5% for the weakest measured lines to about 10% for the strongest lines, and produce linewidth uncertainties that are roughly equivalent to the instrument profile uncertainty (≈0.05 cm^{-1}). For narrow features, the uncertainties in the literature values of the linewidths produce very small uncertainties in our measured f values, typically less than 1%. The total uncertainties in individual line f values from all sources, including statistical uncertainties of the fitting parameters (typically $<10\%$), are estimated to range from 10% to 30%. For any one line in a given band, the f values derived from separate absorption scans were generally found to scatter within narrower limits. Linewidth uncertainties for the five bands with measurably broadened features vary quite widely, depending on the quality of the data and the relative widths of the lines; these uncertainties are discussed separately for each band.

The relative vibronic band strengths of the $(b,c_3,o_3)^1\Pi_u$ and $(b',c_4',c_5')^1\Sigma_u^+$ states calculated by Stahel *et al.*[14] and by Spelsberg and Meyer[19] are derived from models that do not account for rotational interactions. Comparisons of experimental results with the predictions of these spectroscopic models are strictly valid only for rotationless transitions. For some of the bands measured in this study, the rotational line f values follow the simple patterns associated with unper-

turbed transitions. In particular, for unperturbed $^1\Sigma - ^1\Sigma$ and $^1\Pi - ^1\Sigma$ transitions, the band oscillator strength f is related to rotational line oscillator strengths $f_{J',J''}$ by[51]

$$^1\Sigma - ^1\Sigma: \quad f = \frac{(2J''+1)f_{J',J''}}{S_{J',J''}}, \tag{3}$$

$$^1\Pi - ^1\Sigma: \quad f = \frac{2(2J''+1)f_{J',J''}}{S_{J',J''}}, \tag{4}$$

where the $S_{J',J''}$ are the Hönl-London factors. For unperturbed bands, the band f values derived from the application of Eqs. (3) and (4) to measured line f values are independent of the rotational quantum number J and can be directly compared with theoretical results that neglect all rotational interactions.

Most bands in this study display anomalous P-, Q-, and R-branch intensity patterns and are characterized by a marked J dependence of band f values derived from Eqs. (3) and (4). The detailed f-value patterns associated with specific bands are presented in Sec. IV. For transitions from the ground state of N_2, it has to be the upper-state wave function that is responsible for all departures from the standard line-strength formulas.

Accordingly, the band f values derived from Eqs. (3) and (4) are considered as functions of J'. To facilitate comparisons with calculated band strengths, we represent the derived band $f(J')$ values as simple polynomials in $J'(J'+1)$ that are to be used for extrapolation to $J'=0$. For simplicity, we will refer to the band f values extrapolated to $J'=0$ as "rotationless" band f values. Four bands display a J dependence of their linewidths and/or different widths associated with the e- and f-parity levels in the upper state. The J dependences of these linewidths are also represented as simple polynomials in $J'(J'+1)$.

The least-squares fitting routine was not applied to partly blended pairs or groups of lines because of its sensitivity to the exact positions and relative strengths of the lines. To check the overall consistency of our f-value and linewidth results and the validity of interpolations and extrapolations of those results within each band, synthetic room-temperature absorption spectra were generated and compared with our measurements.

IV. RESULTS AND DISCUSSION

A band-by-band summary of our measurements and analyses is presented in Table I. With the exceptions of the very weak transitions to $v=0$, 2, and 3 of the b' state, all electric dipole-allowed N_2 transitions between 93.5 and 99.5 nm are covered in the current survey. For completeness, the table includes the corresponding data for the $c_4'(0)-X(0)$ band, for which line oscillator strengths were published separately by Stark *et al.*[30] A detailed listing of measured f values and widths for individual rotational lines can be accessed through the EPAPS data depository of AIP.[53] Our determinations of line parameters within specific bands, and the rotational dependences of those parameters, will be discussed later in this section.

Table II compares the rotationless band f values of the second column with our earlier *measurements* of selected bands,[29,30] as well as with band f values derived from electron-energy-loss measurements,[18,31] electron-impact studies of emission-excitation cross sections,[32] and calculations based on sets of electronically coupled diabatic potential curves.[14,19] Except for the present work and the calculated f values in the last two columns, all other data in the table are strictly valid only for a room-temperature distribution of rotational populations. Earlier optical-absorption surveys of Carter,[23] Gürtler *et al.*,[24] and Lawrence *et al.*[25] are not included in the table. These studies suffer from inadequate spectral resolution and, thus, systematically underestimate the band f values.

With some exceptions, our rotationless band f values are consistent with the normalized f values of Geiger and Schröder.[18] Notable differences are found for $c_4'(1)-X(0)$ and $c_3(1)-X(0)$; the discrepancies arise from the difficulties of resolving the two transitions in the relatively low-resolution electron-energy-loss spectrum. A significant disagreement is also seen in the oscillator strengths of the very weak $o_3(0)-X(0)$ band, where the Geiger and Schröder[18] result exceeds by almost a factor of three the f value reported by us, probably the consequence of the exceptionally strong J dependence of the line strengths (see Table I) characterizing this band.

The f values proposed by Chan *et al.*[31] are consistently higher than our results. Again, the low resolution of the electron scattering spectra ($\sim$400 cm^{-1}) may explain some of the discrepancies. For example, the extraction of f values for the three overlapping transitions $c_3(0)-X(0)$, $c_4'(0)-X(0)$, and $b(5)-X(0)$ requires the deconvolution of three totally blended peaks of the electron scattering spectrum (see Fig. 4 of Ref. 31). A similar resolution problem exists for the overlapping $c_3(1)-X(0)$, $c_4'(1)-X(0)$, and $b(7)-X(0)$ bands.

Our rotationless band f values can be directly compared with the calculations of Stahel *et al.*[14] and of Spelsberg and Meyer,[19] neither of which accounts for rotational interactions. Table II and Figs. 3(a) and 3(b) show the agreement to be very satisfactory. Clear inconsistencies appear for only two bands, $b(8)-X(0)$ and $o_3(0)-X(0)$, which are among the weakest features in the 93.5–99.5 nm spectral region. As the relative vibronic transition moments of Stahel *et al.*[14] were optimized by fitting the squared moments to the electron-energy-loss spectra of Geiger and Schröder,[18] and since the latter represent measurements over *room-temperature* rotational populations, some departures from measured rotationless f values might be expected.

The current study provides information on the J dependences of band oscillator strengths derived from individual line f values. It also reports the J dependences of linewidths within individual bands. While the f values and linewidths of some bands show a nearly unperturbed behavior, others exhibit extreme departures from the unperturbed patterns. The rather high density of vibronic levels at energies approaching the threshold region and the strength of the Rydberg-Rydberg, Rydberg-valence, and valence-valence interactions make it unlikely that the observations can be fully explained by two- or three-state interactions. A more global modeling approach is needed, such as that undertaken by Lewis *et al.*[22]

TABLE I. Summary of measured f values and linewidths for EUV transitions from $X(0)$ of $^{14}N_2$. Uncertainties (in parentheses) are in units of the last-quoted decimal place. The measured oscillator strengths are reported in terms of a "rotationless" band f value $f(J'=0)$ and a polynomial in $x=J'(J'+1)$ that represents the rotational dependence of band f values $f(J')$ derived from line f values. Analogous parameters, $\Gamma(J'=0)$ and $\Gamma(J')$, are used to report the Lorentzian components (FWHM) of the measured linewidths. Γ_{lit} refers to data taken from literature (Refs. 36–41).

Band	T (cm^{-1})	Lines	Observed J' range	$f(J'=0)$ ($\times 10^3$)	$f(J')$ ($\times 10^3$)	$\Gamma(J'=0)$ (cm^{-1})	$\Gamma(J')$ (cm^{-1})	Γ_{lit} (cm^{-1})
$b(0)-X(0)$	100 817	9	5–13	2.4(2)	2.4(2)			0.17
$b(1)$	101 452	8	9–16	8.1(10)	8.1(10)			0.020
$b(2)$	102 152	27	5–23	21(2)	$20.9-0.0084x$	0.60(7)	$0.60-0.0010x$	
$b(3)$[a]	102 864							
$b(4)$	103 549	45	3–26	68(7)	$67.7-0.034x$	0.30(5)	0.30(5)	
$c_3(0)$	104 139	56	2–27	47(5)	Q: $47.2+0.024x$			0.080
					P: $47.2-0.25x+(9.0\times10^{-4})x^2-(8.7\times10^{-7})x^3$			
					R: $47.2+0.28x-(5.7\times10^{-4})x^2+(83.8\times10^{-7})x^3$			
$c_4'(0)$[b]	104 323	48	0–25	138(14)	P: $138+(6.7\times10^{-2})x$			0.0072
					R: $138-(2.6\times10^{-1})x$			
$b'(1)$[c]	104 419	16	1–11	0.45(9)	$0.45+(8\times10^{-3})x$			0.0086
$b(5)$	104 700	45	1–22	2.8(3)	Q: $2.80+0.018x+(3.0\times10^{-5})x^2$			0.023
					P: $2.80+0.045x+(2.2\times10^{-4})x^2$			
					R: $2.80-0.0015x+(4.0\times10^{-5})x^2$			
$b(6)$	105 346	26	1–14	4.0(4)	Q: $4.00-0.0062x$			0.016
					P: $4.00-0.012x$			
					R: $4.00-0.0022x$			
$o_3(0)$	105 683	12	2–20	0.13(2)	Q: $0.129+0.026x$			0.022
$b(7)$	106 111	45	3–21	17(2)	$16.5-0.016x$			0.0096
$c_4'(1)$	106 370	10	2–13	5.2(6)	P: $5.2-(1.6\times10^{-2})x$			0.016
$c_3(1)$[d]	106 528	22	3–20	36(4)	36(4)		[e]	0.034[f]
$b'(4)$	106 647	13	0–10	1.8(2)	P: $1.8+(3.6\times10^{-3})x$		[g]	
					R: $1.8-(2.8\times10^{-2})x+(1.7\times10^{-4})x^2$			
$b(8)$[h]	106 933	11	4–26	0.44(10)	$0.44-0.003x$			0.056

[a]Line broadening precludes fits to individual lines (see Sec. IV).
[b]Data taken from Ref. 30; polynomial fits are valid for $J\leqslant 10$ (see Sec. IV).
[c]Intensities increase dramatically for $J>7$ owing to the interaction with $c_4'(0)$; polynomial fit is valid for $J<5$.
[d]Anomalous Q-branch intensities for $J>13$ (see Sec. IV).
[e]Q lines broaden significantly for $J>10$, reaching a maximum width of ~ 1.1 cm^{-1} for $J=18$ (see Sec. IV).
[f]Low-J levels only (see Ref. 62 and Sec. IV).
[g]Anomalous linewidth pattern (see Sec. IV).
[h]Anomalous intensity distribution. Polynomial fit is valid for $J<9$ (see Sec. IV).

in their recent description of N_2 predissociation mechanisms. The J dependences found in the present work should help inform future models that include rotational interactions. The following paragraphs provide a band-by-band summary and a discussion of our observations in the 93.5–99.5 nm region.

(1) $b(0)-X(0)$ and $b(1)-X(0)$. Within the limited range of J values measured, no rotational dependence is seen in the band f values extracted from measured line f values in these two bands. This is consistent with the relatively isolated positions of $b(0)$ and $b(1)$ and the fact that their wave functions are of nearly pure-b-state character.[47] The Lorentzian contribution to the linewidths in the $b(1)-X(0)$ band, whose upper state is known to fluoresce,[54] is far too narrow to be observed with our apparatus. We see some evidence of broadening of the $b(0)-X(0)$ lines in our measurements, but the fitting uncertainties are unacceptably large; lifetime measurements[41] were used to fix the Lorentzian width at 0.17 cm^{-1} in our analysis.

(2) $b(2)-X(0)$. A weak J dependence is observed in the band f values derived from line oscillator strengths. More significantly, the Lorentzian component of the linewidth in all branches is found to vary dramatically, decreasing from ≈ 0.58 cm^{-1} for $J'=0$ to about 0.10 cm^{-1} at $J'=22$. The linewidth data are displayed in Fig. 4. Ubachs *et al.*[34] reported a Lorentzian width of 0.53 cm^{-1} for $R(12)$, marginally consistent with 0.41 cm^{-1} for $J'=13$ from a linear fit to our measurements. Lewis *et al.*[22] performed a coupled-Schrödinger-equation calculation ($^1\Pi_u$ and $^3\Pi_u$ states only) for nonzero J values that qualitatively reproduces the J-dependent level broadening pattern for the $b(2)$ state. As pointed out by Stevens *et al.*,[5,6] the strongly predissociating $b(2)-X(0)$ band plays an important role in multiple-scattering models of terrestrial and planetary airglows because of its overlap with the $c_4'(0)\rightarrow X(1)$ emission. Line profiles in $b(2)-X(0)$ influence the loss of airglow photons through reabsorption by N_2; including the strong J dependence of the line profiles should improve the reliability of multiple-scattering models.

(3) $b(3)-X(0)$. The $b(3)$ upper state is marked by very strong predissociation, resulting in unusually diffuse rotational features. Most lines in the band are at least partially blended, and there is a significant overlap be-

TABLE II. Comparison of band oscillator strengths ($\times 10^3$) for EUV transitions of $^{14}N_2$. Uncertainties (in parentheses) are in units of the last quoted decimal place. The band f values of column 2 are "rotationless" with the exception of the value for $b(3)-X(0)$; the latter and f values in columns 3–6 are strictly appropriate for room temperature only.

Band	This work	Stark *et al.*[a,b]	Ref. 18[c]	Ref. 31[d]	Ref. 32	Ref. 14[c]	Ref. 19[c]
$b(0)-X(0)$	2.4(2)	2.2(2)	1.8	2.5		2.0	2.3
$b(1)$	8.1(10)	9.6(10)	11	11		9.1	9.6
$b(2)$	21(2)	22(2)	23	27		23	23
$b(3)$	43(6)[e]	51(5)	43	53		43	43
$b(4)$	68(7)	61(6)	68	86		59	65
$c_3(0)$	47(5)	56(8)	49	64		44	49
$c_4'(0)$	138(14)	145(28),[a] 136(20)[b]	159	195	156	143	140
$b'(1)$	0.45(9)					0.49	0.48
$b(5)$	2.8(3)		3.5	6.1		2.5	3.0
$b(6)$	4.0(4)		3.0	5.0		3.8	5.5
$o_3(0)$	0.13(2)		0.35			0.99	0.46
$b(7)$	17(2)		18	24		21	20
$c_4'(1)$	5.2(6)		1.5	1.5	3.8	8.3	6.4
$c_3(1)$	36(4)		50	64		35	36
$b'(4)$	1.8(2)					2.1	2.0
$b(8)$	0.44(10)		0.35			1.5	0.9

[a]Reference 29.
[b]Reference 30.
[c]f-values normalized to $f=0.043$ for $b(3)-X(0)$.
[d]Uncertainties $\sim 10\%$.
[e]Room-temperature f value.

tween lines in the P and Q branches. Consequently, our fitting procedure for individual spectral lines was not applied, and no oscillator strengths or widths of individual lines have been evaluated. From an integration over the entire band, the room temperature band f value is determined to be 0.043(6), somewhat lower than our earlier reported value of 0.051(5).[29] Lewis *et al.*[22] attribute the large width of $b(3)$ to a spin-orbit interaction with the nearly degenerate $C\,^3\Pi_u(v=9)$ level, which, in turn, strongly predissociates into the continuum of $C'\,^3\Pi_u$. The accompanying paper by Haverd *et al.*[48] applies refinements of the coupled-Schrödinger-equation model of Lewis *et al.*[22] to a detailed analysis of $b(3)-X(0)$ that includes the rotational dependence of the linewidths and line strengths.

(4) $b(4)-X(0)$. Band f values derived from line f values appear to decrease with increasing rotational quantum number. There is also some indication that the P/R ratio of line f values is consistently lower, by about 20%, than what is expected for an unperturbed line-strength distribution. The rotational linewidths are significant but vary minimally with J and are comparable for lines terminating on the e- and f-parity levels of $b(4)$. The width of 0.30(6) cm^{-1}, valid for all rotational lines, is in very good agreement with the value reported by Ubachs *et al.*[37] (0.29 cm^{-1}) for low-J lines. The coupled-Schrödinger-equation model of Lewis *et al.*[22] correctly reproduces the minimal J dependence of the linewidths. The $R(17)$ and $P(19)$ lines of $b(4)-X(0)$ are displaced by ~ 1.4 cm^{-1} from their expected positions to lower energies, and two extra lines are observed symmetrically displaced to higher energies. About 40% of the expected strength of the affected lines has shifted to the extra lines, a clear indication that the e-parity $J=18$ levels of $b(4)$ is perturbed. The $Q(18)$ line is not affected. This perturbation was also noted by Sprengers *et al.*[55] in $^{14}N_2$ and at $J=15$ of $^{15}N_2$. A clear identification of the perturber state has not been made.

(5) $c_4'(0)-X(0)$ and $c_3(0)-X(0)$. The $c_4'(0)\,^1\Sigma_u^+$ and $c_3(0)\,^1\Pi_u$ levels form part of the lowest $3p$ complex of N_2, and the respective transitions from $X(0)$ account for two of the strongest features in the EUV spectrum. The absorption signatures of both bands were recently identified in the interstellar medium.[8] The $c_4'(0)$ level plays a central role in atmospheric emission studies and has been thoroughly investigated by a number of authors.[30,38,45–47,56,57] The line f values for 48 lines in the $c_4'(0)-X(0)$ band were reported by Stark *et al.*[30] The P/R ratios of the f values were found to be consistently larger, by about 20%, than the ratios predicted from simple Hönl-London factors, in qualitative agreement with the description of $c_4'(0)$ as the upper component of a Rydberg p complex.[58,59] Our new results for the R and P branches of the $c_3(0)-X(0)$ band show a complementary behavior for the lower component of the p complex (see Fig. 5). Any quantitative analysis of the line-strength patterns in the two bands will have to take into account the strong mixing of $c_3(0)$ with the $b\,^1\Pi_u$ valence state, particularly with $b(4)$ and $b(5)$.[14,47] Further complications arise from the avoided crossing of $c_4'(0)$ with $b'(1)$ at $J\approx 11$ (Refs. 56 and 57) and from

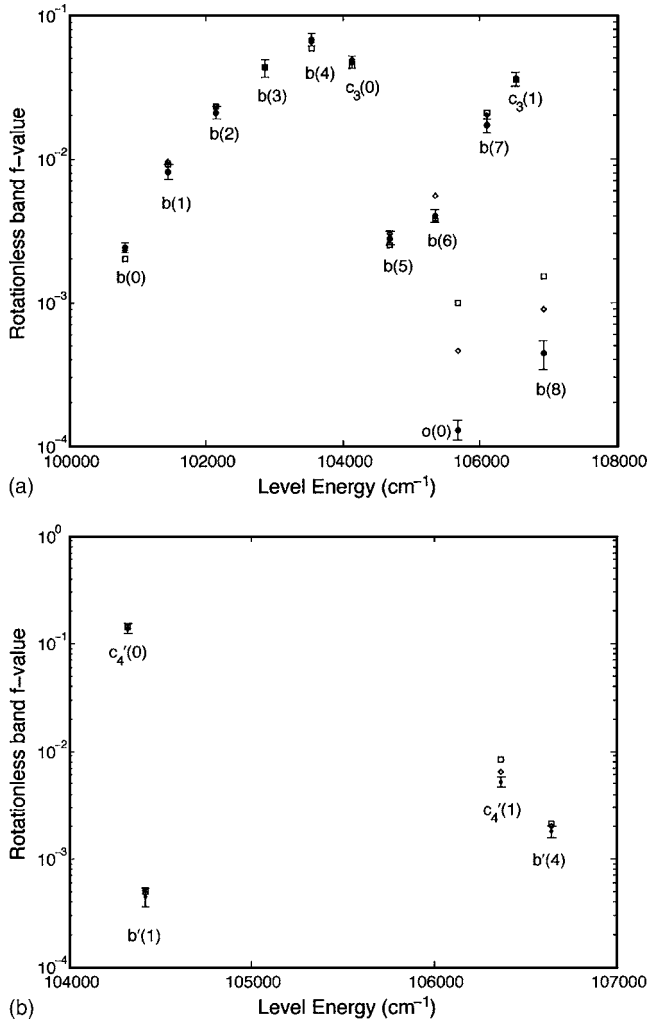

FIG. 3. Comparisons between our experimental rotationless band f values (solid circles with uncertainties) and calculated f values [Stahel *et al.* (Ref. 14)-solid circles; Spelsberg and Meyer (Ref. 19)-open diamonds] for (a) $^1\Pi_u \leftarrow X\,^1\Sigma_g^+$ bands and (b) $^1\Sigma_u^+ \leftarrow X\,^1\Sigma_g^+$ bands. The calculated f values have been normalized to $f=0.043$ for the $b(3)-X(0)$ band.

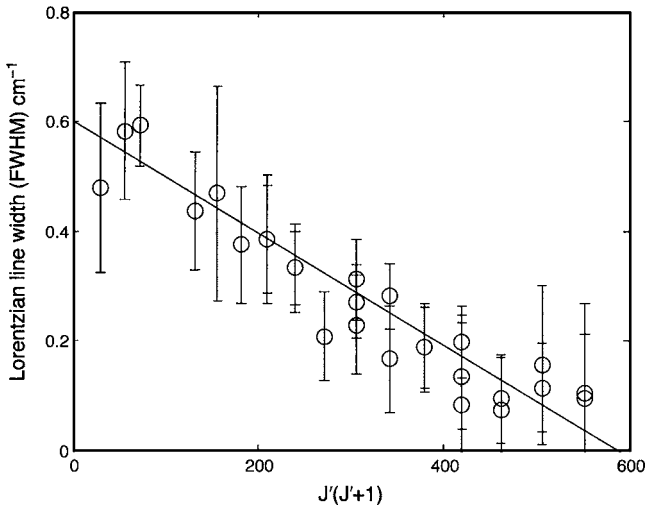

FIG. 4. Experimentally determined Lorentzian component of linewidths (FWHM) in the $b(2)-X(0)$ band (open circles) and linear fit to $J'(J'+1)$.

the long-range interference of $c_4'(0)$ with the entire $b'(v)$ progression (see Ref. 30).

(6) A linear fit of $c_3(0)-X(0)$ band f values, derived from Q-branch line f values, to $J'(J'+1)$ yields a rotationless band f value of 0.047(5). In subsequent fits of the P- and R-branch f values, the rotationless band oscillator strength was held fixed at this value. Cubic fits were required to reproduce the P- and R-branch f-value patterns, reflecting the rapid onset of the J-dependent interaction with the $c_4'(0)$ level. These higher-order polynomial fits should not be extrapolated beyond the range of J values presented in our data compilation. Line broadening effects in the $c_3(0)-X(0)$ band could not be directly observed in our spectra; the Lorentzian component of all linewidths was held fixed at 0.08 cm^{-1}, as determined from recent laser-based linewidth measurements.[41] Our rotationless band f value, along with the J dependence of the line f values in the P, Q, and R branches, leads to a room-temperature band f value of 0.052, quite consistent with our earlier result of 0.056(8).[29]

(7) $b'(1)-X(0)$. The rotationless f value of the weak $b'(1)-X(0)$ band was determined from a linear fit of measured f values vs $J'(J'+1)$ for $J'<5$. Beyond these lowest rotational levels, the onset of the interaction between $b'(1)$ and $c_4'(0)$[56,57] very quickly results in the $b'(1)-X(0)$ lines gaining significant strength. Six rotational line f values, with $J'>7$, were reported earlier;[30] they were not included in the rotationless f-value determination.

(8) $b(5)-X(0)$. Line f-value patterns in this band deviate significantly from those predicted by $^1\Pi-{}^1\Sigma$ Hönl-London factors (see Fig. 6). The most striking features are the rapidly increasing strength of the P-branch lines with increasing rotational quantum number and the relative weakness of the R-branch lines. At low J values, the band f values derived from lines within the P, Q, or R branches converge to a common rotationless

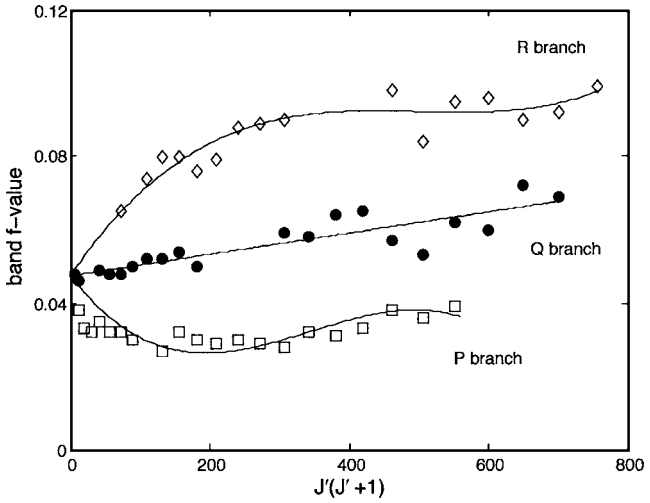

FIG. 5. $c_3(0)-X(0)$ band f values determined from rotational line f values and Hönl-London factors (P branch-open squares, Q branch-solid circles, and R branch-open diamonds). The J dependence of the Q-branch f values is adequately represented by a linear fit to $J'(J'+1)$; P-branch and R-branch f values are fit to higher-order polynomials with a common rotationless intercept.

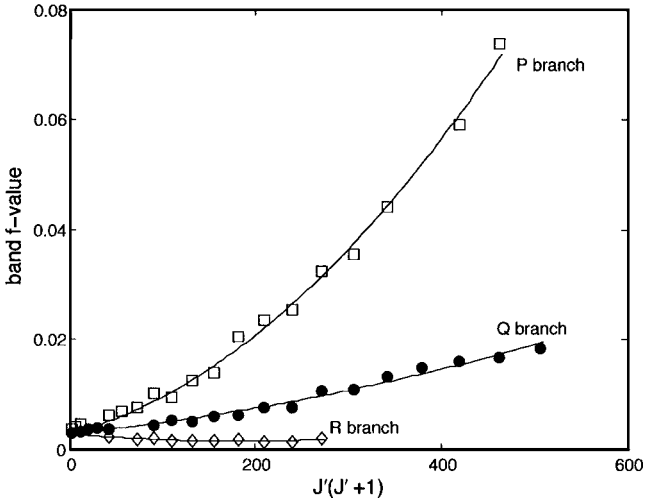

FIG. 6. $b(5)-X(0)$ band f values determined from rotational line f values and Hönl-London factors (P branch-open squares, Q branch-solid circles, and R branch-open diamonds). The J dependences of the f values in the three branches are fit to quadratics (solid lines) with a common rotationless intercept.

value of 0.002 8(3). For $J'>10$, P-line f values are larger than the corresponding Q-line f values, and band f values derived from the highest-J P lines are as much as a factor of 20 times larger than the rotationless band f value. The $b(5)$ level is strongly mixed with the $3p\pi$ $c_3(0)$ level and to a lesser extent with o_3,[47] enabling the e-parity levels of $b(5)$ to assume a c_4' $3p\sigma$ character that grows quickly with J (see Fig. 2 of Edwards *et al.*[47]). The increased intensity of the P branch is borrowed from the $c_4'(0)-X(0)$ transition, and the large discrepancies between R- and P-branch intensities mirrors the l-uncoupling interaction within the $3p$ complex.

(9) $b(6)-X(0)$. The band f values derived from the branches of this sharp band converge to a common rotationless f value and were fit separately to linear functions of $J'(J'+1)$. The P/R ratios of the line f values deviate somewhat from predictions based on Hönl-London factors, though not dramatically. The line f values for P and R transitions from a common J'' level add up to the f value for the corresponding Q line.

(10) $o_3(0)-X(0)$. This was the weakest band measured in our survey, and only a limited number of rotational lines were analyzed. A linear fit of the f values of nine lines in the Q branch vs $J'(J'+1)$ yields a rotationless band f value of 0.000 13(2) and shows the band f value to increase with J. Only fragmentary information on P- and R-branch f values is obtained, and it is not evident that these data are consistent with the Q-branch results. Yoshino *et al.*[60] describe two perturbations of the $o_3(0)$ level, a heterogeneous interaction with $b'(3)$ and a homogeneous interaction with $b(7)$ at high J values. Our data are not complete enough to observe any corresponding effects on line strengths.

(11) $b(7)-X(0)$. The rotational structure of this band allows for a fairly complete set of line f-value measurements in all three branches; a total of 45 line f values were determined. All band f values determined from line f values follow the same linearly decreasing function of $J'(J'+1)$. The homogeneous interaction of $b(7)$ with the ower energy $o_3(0)$ level[13,60] which has a larger-B value, qualitatively explains the diminishing strength with increasing J of the $b(7)-X(0)$ lines in all three branches. The absence of noticeable Λ-type doubling[13] indicates the weakness of any heterogeneous interactions and is consistent with the fact that the P/R ratios of the line f values are governed by simple Hönl-London factors.

(12) $c_4'(1)-X(0)$. This band is overlapped by the stronger $c_3(1)-X(0)$ band, and only ten P-line f values could be measured. The band f values derived from these measurements were fit to a linearly decreasing function of $J'(J'+1)$. R-branch lines are either blended with $c_3(1)-X(0)$ features or too weak to be measured. However, comparisons of a synthetic band model with our measured spectra indicate that the R lines may be stronger than predicted by Hönl-London factors. Yoshino *et al.*[61] and Ubachs *et al.*[38] discuss the spectroscopy of $c_4'(1)$ and identify a strong homogeneous interaction with $b'(4)$. Figure 6 of Ref. 38 shows that for $J\approx 16$, $c_4'(1)$ has nearly 50% b' [mainly $b'(4)$] fractional vibronic character. The decrease in line strength with increasing rotation can be qualitatively explained by this growing interaction, the $b'(4)-X(0)$ transition being significantly weaker than $c_4'(1)-X(0)$. A complementary trend is observed for $b'(4)-X(0)$.

(13) $c_3(1)-X(0)$. For $J'<14$, the band f values derived from P, Q, and R lines are all very similar and J independent. For higher J, the Q-branch lines, which could be followed to $J=20$, display a clear intensity anomaly, with peak strengths at $J'=17-18$ that exceed by a factor of two the line strengths observed for low rotational quantum numbers. The anomaly in the Q branch is accompanied by significant line broadening. Below $J'=11$, no broadening is observed with our apparatus. The Q lines, from $Q(11)$ through $Q(20)$, are noticeably broader, the linewidths peaking at ≈ 1.1 cm^{-1} for $J=17-18$ and dropping to ≈ 0.8 cm^{-1} for $J=20$. Linewidths for rotational levels up to $J_f=16$ and $J_e=13$ were previously reported by Kawamoto *et al.*[62] in a near-infrared diode laser study of the $c_3\,{}^1\Pi_u-a''\,{}^1\Sigma_g^+$1-0 band; the Q-branch linewidths were found to increase approximately linearly with $J'(J'+1)$, and they agree, in the region of overlap, with our own measurements. The same authors also report broadening in the R and P branches, an observation which we cannot confirm. Measurements of Sprengers *et al.*[40] indicate a shortening of the radiative lifetime in the $c_3(1)$ level with increasing J. Although individual lines could not be resolved, their observations are broadly consistent with the results of Kawamoto *et al.*[62] and with our results.

(14) $b'(4)-X(0)$. This band is characterized by a strong P branch and a much weaker R branch. With increasing J', the P branch grows in intensity faster than expected on the basis of Hönl-London factors. The band f values derived from the P lines were first fit to a linear func-

tion of $J'(J'+1)$ to yield the rotationless band f value. The corresponding R-branch data were then fit to a quadratic function with the $J'=0$ intercept held fixed at the rotationless band f value. Line broadening is seen in both branches beginning at $J'\approx 5$; the broadening peaks with a width of ≈ 0.8 cm^{-1} for $J'\approx 7$.

(15) $b(8)-X(0)$. The unusual line-strength anomaly in this band was first reported by Carroll and Collins.[13] The line intensities in all three branches drop precipitously for $J'>10$: they are indiscernible, in our scans, for $J'=12$ and 13, and reappear with significant strength in all three branches for higher J values. A related intensity pattern is observed in $^{15}N_2$ at lower J values,[54] the pattern being ascribed to a destructive interference between Rydberg and valence $^1\Pi_u$ transition amplitudes. Five low-J Q-line f values are used to determine the rotationless band f value.

As part of this work, a photographic plate of the room-temperature absorption through a high column density of N_2 (Ref. 63) was used to extend the $b(8)-X(0)$ analysis of Carroll and Collins[13] to lines beyond the region of destructive interference. The measured wavelengths, upper-state term values, and derived molecular parameters for $b(8)$ are summarized in Tables XVI and XVII of the data archive sent to the EPAPS depository of AIP.[53] The f values of four high-J Q lines lying within the adjacent $b'(4)-X(0)$ band were measured; they confirm the sharp increase in line strengths above the region of destructive interference predicted by the model of Haverd *et al.*[48]

ACKNOWLEDGMENTS

This work was supported in part by NASA Grants No. NAG5-9059 and No. NNG05GA03G to Wellesley College. The measurements were carried out under the approval of the Photon Factory Advisory Committee (Proposal No. 1998G245); we thank the staff of the Photon Factory for their hospitality and assistance. We also thank Brenton Lewis for his valuable comments and for help with extracting $b(8)$ molecular parameters from the revised line list.

[1] R. R. Meier, Space Sci. Rev. **58**, 1 (1991).
[2] P. D. Feldman, D. J. Sahnow, J. W. Kruk, E. M. Murphy, and H. W. Moos, J. Geophys. Res. **106**, 8119 (2001).
[3] J. Bishop and P. D. Feldman, J. Geophys. Res. **108**, 1243 (doi: 10.1029/2001JA000330, 2003).
[4] D. F. Strobel and D. E. Shemansky, J. Geophys. Res. **87**, 1361 (1982).
[5] M. H. Stevens, R. R. Meier, R. R. Conway, and D. F. Strobel, J. Geophys. Res. **99**, 417 (1994).
[6] M. H. Stevens, J. Geophys. Res. **106**, 3685 (2001).
[7] A. L. Broadfoot *et al.*, Science **246**, 1459 (1989).
[8] D. C. Knauth, B.-G. Andersson, S. R. McCandliss, and H. W. Moos, Nature (London) **429**, 636 (2004).
[9] L. E. Young, G. Stark, and R. J. Vervack, Bull. Am. Astron. Soc. **34**, 878 (2002).
[10] R. J. Vervack, B. R. Sandel, and D. F. Strobel, Icarus **170**, 91 (2004).
[11] H. Lefebvre-Brion, Can. J. Phys. **47**, 541 (1969).
[12] K. Dressler, Can. J. Phys. **47**, 547 (1969).
[13] P. K. Carroll and C. P. Collins, Can. J. Phys. **47**, 563 (1969).
[14] D. Stahel, M. Leoni, and K. Dressler, J. Chem. Phys. **79**, 2541 (1983).
[15] P. K. Carroll, C. P. Collins, and K. Yoshino, J. Phys. B **3**, L127 (1970).
[16] P. K. Carroll and K. Yoshino, J. Phys. B **5**, 1614 (1972).
[17] K. Yoshino, Y. Tanaka, P. K. Carroll, and P. Mitchell, J. Mol. Spectrosc. **54**, 87 (1975).
[18] J. Geiger and B. Schröder, J. Chem. Phys. **50**, 7 (1969).
[19] D. Spelsberg and W. Meyer, J. Chem. Phys. **115**, 6438 (2001).
[20] M. Leoni and K. Dressler, Z. Angew. Math. Phys. **22**, 794 (1971).
[21] J. M. Robbe, Ph.D. thesis, University of Lille, 1978.
[22] B. R. Lewis, S. T. Gibson, W. Zhang, H. Lefebvre-Brion, and J.-M. Robbe, J. Chem. Phys. **122**, 144302 (2005).
[23] V. L. Carter, J. Chem. Phys. **56**, 4195 (1972).
[24] P. Gürtler, V. Saile, and E. E. Koch, Chem. Phys. Lett. **48**, 245 (1977).
[25] G. M. Lawrence, D. L. Mickey, and K. Dressler, J. Chem. Phys. **48**, 1989 (1968).
[26] R. D. Hudson, Rev. Geophys. **9**, 305 (1971).
[27] G. Stark, K. Yoshino, P. L. Smith, K. Ito, and W. H. Parkinson, Mater. Sci. Monogr. **369**, 574 (1991).
[28] W. F. Chan, G. Cooper, and C. E. Brion, Phys. Rev. A **44**, 186 (1991).
[29] G. Stark, P. L. Smith, K. P. Huber, K. Yoshino, M. H. Stevens, and K. Ito, J. Chem. Phys. **97**, 4809 (1992).
[30] G. Stark, K. P. Huber, K. Yoshino, M. C. Chan, T. Matsui, P. L. Smith, and K. Ito, Astrophys. J. **531**, 321 (2000).
[31] W. F. Chan, G. Cooper, R. N. S. Sodhi, and C. E. Brion, Chem. Phys. Lett. **170**, 81 (1993).
[32] J. M. Ajello, G. K. James, B. O. Franklin, and D. E. Shemansky, Phys. Rev. A **40**, 3524 (1989).
[33] H. Oertel, M. Kratzat, J. Imschweiler, and T. Noll, Chem. Phys. Lett. **82**, 552 (1981).
[34] W. Ubachs, L. Tashiro, and R. N. Zare, Chem. Phys. **130**, 1 (1989).
[35] W. Ubachs, K. S. F. Eikema, and W. Hogervorst, Appl. Phys. B **57**, 411 (1993).
[36] W. Ubachs, Chem. Phys. Lett. **268**, 201 (1997).
[37] W. Ubachs,I. Velchev, and A. de Lange, J. Chem. Phys. **112**, 5711 (2000).
[38] W. Ubachs, R. Lang, I. Velchev, W.-U. L. Tchang-Brillet, A. Johansson, Z. X. Li, V. Lokhnygin, and C.-G. Wahlström, Chem. Phys. **270**, 215 (2001).
[39] J. P. Sprengers, W. Ubachs, A. Johansson, A. L'Huillier, C.-G. Wahlström, R. Lang, B. R. Lewis, and S. T. Gibson, J. Chem. Phys. **120**, 8973 (2004).
[40] J. P. Sprengers, A. Johansson, A. L'Huillier, C.-G. Wahlström, B. R. Lewis, and W. Ubachs, Chem. Phys. Lett. **389**, 348 (2004).
[41] J. P. Sprengers, W. Ubachs, and K. G. H. Baldwin, J. Chem. Phys. **122**, 144301 (2005).
[42] C. W. Walter, P. C. Cosby, and H. Helm, J. Chem. Phys. **112**, 4621 (2000).
[43] H. Helm, I. Hazell, and N. Bjerre, Phys. Rev. A **48**, 2762 (1993).
[44] J. M. Ajello, G. K. James, and M. Ciocca, J. Phys. B **31**, 2437 (1998).
[45] D. E. Shemansky, I. Kanik, and J. M. Ajello, Astrophys. J. **452**, 480 (1995).
[46] X. Liu, D. E. Shemansky, M. Ciocca, I. Kanik, and J. M. Ajello, Astrophys. J. **623**, 579 (2005).
[47] S. A. Edwards, W.-U. L. Tchang-Brillet, J.-Y. Roncin, F. Launay, and F. Rostas, Planet. Space Sci. **43**, 67 (1995).
[48] V. E. Haverd, B. R. Lewis, S. T. Gibson, and G. Stark, J. Chem. Phys. **123**, 214304 (2005), following paper.
[49] K. Ito, T. Namioka, Y. Morioka, T. Sasaki, H. Noda, K. Goto, T. Katayama, and M. Koike, Appl. Opt. **25**, 837 (1986).
[50] K. Ito, K. Maeda, Y. Morioka, and T. Namioka, Appl. Opt. **28**, 1813 (1989).
[51] D. C. Morton and L. Noreau, Astrophys. J., Suppl. Ser. **95**, 301 (1994).
[52] S. A. Edwards, J.-Y. Roncin, F. Launay, and F. Rostas, J. Mol. Spectrosc. **162**, 257 (1993).
[53] See EPAPS Document No. E-JCPSA6-123-020544. This data archive consists of tabulations of experimentally determined line f values and linewidths in 15 $^{14}N_2$ bands between 93.5 and 99.5 nm. Tables of line positions in the $b(8)-X(0)$ band and molecular parameters for the $b(8)$ level are also included. This document can be reached via a direct link in the online article's HTML reference section or via the EPAPS homepage (http://www.aip.org/pubservs/epaps.html).
[54] J.-Y. Roncin and F. Launay, Astron. Astrophys., Suppl. Ser. **128**, 361 (1998).
[55] J. P. Sprengers, W. Ubachs, K. G. H. Baldwin, B. R. Lewis, and W.-Ü. L. Tchang-Brillet, J. Chem. Phys. **119**, 3160 (2003).

[56] K. Yoshino and Y. Tanaka, J. Mol. Spectrosc. **66**, 219 (1977).
[57] P. F. Levelt and W. Ubachs, Chem. Phys. **163**, 263 (1992).
[58] P. K. Carroll, J. Chem. Phys. **58**, 3597 (1973).
[59] J. W. C. Johns, Mol. Spectrosc. (Chem. Soc., London) **2**, 513 (1974).
[60] K. Yoshino, Y. Tanaka, P. K. Carroll, and P. Mitchell, J. Mol. Spectrosc. **54**, 87 (1975).
[61] K. Yoshino, D. E. Freeman, and Y. Tanaka, J. Mol. Spectrosc. **76**, 153 (1979).
[62] Y. Kawamoto, M. Fujitake, and N. Ohashi, J. Mol. Spectrosc. **185**, 330 (1997).
[63] The plate was recorded on the 6.65 m vacuum spectrometer at the Harvard-Smithsonian Center for Astrophysics with a helium continuum light source [K. Yoshino (unpublished)].